The Beaker phenomenon and the genomic transformation of northwest Europe

Citation for published version:
Olalde, I, Brace, S, Allentoft, ME, Armit, I, Kristiansen, KU, Booth, T, Rohland, N, Mallick, SK, Szécsényi-Nagy, A, Mittnik, A, Altena, E, Lipson, M, Lazaridis, I, Harper, TK, Patterson, N, Broomandkhoshbacht, N, Diekmann, Y, Faltyskova, Z, Fernandes, DN, Ferry, M, Harney, E, de Knijff, P, Michel, M, Oppenheimer, J, Stewardson, K, Barclay, A, Alt, KW, Liesau, C, Rios, P, Blasco Romera, C, Miguel, JV, Garcia, MR, Fernandez, AA, Banffy, E, Bernabo-Brea, M, Billoin, D, Bonsall, C, Bonsall, L, Allen, TM, Buster, L, Carver, SJ, Navarro, LC, Craig, OE, Cook, GT, Cunliffe, B, Denaire, A, Dinwiddy, KE, Dodwell, N, Ernee, M, Evans, C, Kucharik, M, Farre, JF, Fowler, AC, Gazenbeek, M, Pena, RG, Haber-Uriarte, M, Haduch, E, Hey, G, Jowett, N, Knowles, TD, Massy, K, Pfrengle, S, Lefranc, P, Lemercier, O, Lefebvre-Schuhl, A, Martinez, CH, Olmo, VG, Ramirez, AB, Maurandi, JL, Majo, T, McKinley, JI, McSweeney, K, Mende, BG, Modi, A, Kulcsar, G, Kiss, V, Czene, A, Patay, R, Endrodi, A, Kohler, K, Hajdu, T, Szeniczey, T, Dani, J, Bernert, Z, Hoole, M, Cheronet, O, Keating, D, Veleminsky, P, Dobe, M, Candilio, F, Brown, F, Fernandez-Santiago, R, Herrero-Corral, A-M, Tusa, S, Carnieri, E, Lentini, L, Valenti, A, Zanini, A, Waddington, C, Delibes, G, Guerra-Doce, E, Neil, B, Brittain, M, Luke, GM, Mortimer, R, Desideri, J, Besse, M, Brucken, G, Furmanek, M, Hauszko, A, Mackiewicz, M, Rapinski, A, Leach, S, Soriano, I, Lillios, KT, Cardoso, JL, Pearson, MP, Wodarczak, P, Price, TD, Prieto, P, Rey, P-J, Risch, R, Guerra, MAR, Schmitt, A, Serralongue, J, Silva, MA, Smrcka, V, Vergnaud, L, Zilhao, J, Caramelli, D, Higham, T, Thomas, MG, Kennett, DJ, Fokkens, H, Heyd, V, Sheridan, A, Sjogren, K-G, Stockhammer, PW, Krause, J, Pinhasi, R, Haak, W, Barnes, I, Lalueza-Fox, C & Reich, D 2018, 'The Beaker phenomenon and the genomic transformation of northwest Europe', *Nature*, vol. 555, no. 7695, pp. 190-196. https://doi.org/10.1038/nature25738

Digital Object Identifier (DOI):
10.1038/nature25738

Published In:
Nature

The Beaker Phenomenon and the Genomic Transformation of Northwest Europe

Iñigo Olalde, Selina Brace, Morten E. Allentoft, Ian Armit*, Kristian Kristiansen*, Nadin Rohland, Swapan Mallick, Thomas Booth, Anna Szécsényi-Nagy, Alissa Mittnik, Eveline Altena, Mark Lipson, Iosif Lazaridis, Thomas K. Harper, Nick Patterson, Nasreen Broomandkhoshbacht, Yoan Diekmann, Zuzana Faltyskova, Daniel Fernandes, Matthew Ferry, Eadaoin Harney, Peter de Knijff, Megan Michel, Jonas Oppenheimer, Kristin Stewardson, Alistair Barclay, Kurt W. Alt, Azucena Avilés Fernández, Eszter Bánffy, Maria Bernabò-Brea, David Billoin, Concepción Blasco, Clive Bonsall, Laura Bonsall, Tim Allen, Lindsey Büster, Sophie Carver, Laura Castells Navarro, Oliver Edward Craig, Gordon T. Cook, Barry Cunliffe, Anthony Denaire, Kirsten Egging Dinwiddy, Natasha Dodwell, Michal Ernée, Christopher Evans, Milan Kuchařík, Joan Francès Farré, Harry Fokkens, Chris Fowler, Michiel Gazenbeek, Rafael Garrido Pena, María Haber-Uriarte, Elżbieta Haduch, Gill Hey, Nick Jowett, Timothy Knowles, Ken Massy, Saskia Pfrengle, Philippe Lefranc, Olivier Lemercier, Arnaud Lefebvre, Joaquín Lomba Maurandi, Tona Majó, Jacqueline I. McKinley, Kathleen McSweeney, Mende Balázs Gusztáv, Alessandra Modi, Gabriella Kulcsár, Viktória Kiss, András Czene, Róbert Patay, Anna Endrődi, Kitti Köhler, Tamás Hajdu, Tamás Szeniczey, János Dani, Maya Hoole, Olivia Cheronet, Denise Keating, Petr Velemínský, Miroslav Dobeš, Francesca Candilio, Fraser Brown, Raúl Flores Fernández, Ana-Mercedes Herrero-Corral, Sebastiano Tusa, Emiliano Carnieri, Luigi Lentini, Antonella Valenti, Alessandro Zanini, Clive Waddington, Germán Delibes, Elisa Guerra-Doce, Benjamin Neil, Marcus Brittain, Mike Luke, Richard Mortimer, Jocelyne Desideri, Marie Besse, Günter Brücken, Mirosław Furmanek, João Luís Cardoso, Corina Liesau, Michael Parker Pearson, Piotr Włodarczak, T. Douglas Price, Pilar Prieto, Pierre-Jérôme Rey, Patricia Ríos, Roberto Risch, Manuel A. Rojo Guerra, Aurore Schmitt, Joël Serralongue, Ana Maria Silva, Václav Smrčka, Luc Vergnaud, João Zilhão, David Caramelli, Thomas Higham, Douglas J. Kennett, Volker Heyd, Alison Sheridan, Karl-Göran Sjögren, Mark G. Thomas, Philipp W. Stockhammer, Johannes Krause, Ron Pinhasi*, Wolfgang Haak*, Ian Barnes*, Carles Lalueza-Fox*, David Reich*

*Principal investigators who contributed centrally to this study

To whom correspondence should be addressed: I.O. (inigo_olalde@hms.harvard.edu) or D.R. (reich@genetics.med.harvard.edu)

Bell Beaker pottery spread across western and central Europe beginning around 2750 BCE before disappearing between 2200–1800 BCE. The forces propelling its expansion are a matter of long-standing debate, with support for both cultural diffusion and migration. We present new genome-wide data from 400 Neolithic, Copper Age and Bronze Age Europeans, including 234 Beaker-associated individuals. We detected limited genetic affinity between Iberian and central European Beaker-associated individuals, and thus exclude migration as a significant mechanism of spread between these two regions. However, migration played a key role in the further dissemination of the Beaker Complex, a phenomenon we document most clearly in Britain where we report 155 individuals who lived from 4000-800 BCE. British Neolithic farmers were genetically similar to contemporary populations in continental Europe and especially to Neolithic Iberians, indicating that a portion of their ancestry came from the Mediterranean rather than the Danubian route of farming expansion. Beginning with the Beaker period, all British individuals in our time transect harboured high proportions of Steppe-related ancestry and were most closely related to Beaker-associated individuals from the Lower Rhine area. The impact of the migration from the continent was profound, as we show that the spread of the Beaker Complex to Britain was associated with a replacement of ~90% of Britain's gene pool within a few hundred years, continuing the east-to-west expansion that had brought Steppe-related ancestry into central and northern Europe 400 years earlier.

During the third millennium Before the Common Era (BCE), two new archaeological pottery styles expanded across Europe, replacing many of the more localized styles that preceded them.[1] In north-central and northeastern Europe there was the 'Corded Ware Complex' associated with people who derived most of their ancestry from Yamnaya pastoralists from the Eurasian steppe[2–4] (henceforth referred to as Steppe). In western Europe there was the equally expansive 'Bell Beaker Complex,' defined by assemblages of grave goods including stylised bell-shaped pots, copper daggers, arrowheads, stone wristguards and V-perforated buttons[5] (Extended Data Fig. 1). The oldest radiocarbon dates associated with Beaker pottery are around 2750 BCE in Atlantic Iberia[6], which has been interpreted as evidence that the Beaker Complex originated there. However, the geographic origin is still debated[7] and other scenarios including an origin in the Lower Rhine or even multiple independent origins are plausible (Supplementary Information section 1). Regardless of the geographic origin, by 2500 BCE the Beaker Complex had spread throughout western Europe (and northwest Africa), and reached southern and Atlantic France, Italy and central Europe[5], where it overlapped geographically with the Corded Ware Complex. Within another hundred years, it had expanded to Britain and Ireland[8]. A major debate in archaeology has revolved around the question of whether the spread of the Beaker Complex was mediated by the movement of people, culture, or a combination[9]. Genome-wide

data have revealed high proportions of Steppe-related ancestry in Beaker Complex-associated individuals from Germany and the Czech Republic[2–4], showing that they derived from mixtures of populations from the Steppe and the preceding farmers of Europe. However, a deeper understanding of the ancestry of people associated with the Beaker Complex requires genomic characterization of individuals across the geographic range and temporal duration of this archaeological phenomenon.

Ancient DNA data

To understand the genetic structure of ancient people associated with the Beaker Complex and their relationship to preceding, subsequent and contemporary peoples, we enriched ancient DNA libraries for sequences overlapping 1,233,013 single nucleotide polymorphisms (SNPs) by hybridization DNA capture[4,10], and generated new sequence data from 400 ancient Europeans dated to ~4700–800 BCE and excavated from 137 different sites (Extended Data Table 1; Supplementary Table 1; Supplementary Information, section 2). This dataset includes Beaker-associated individuals from Iberia (n=45), southern France (n=4), northern Italy (n=3), Sicily (n=3), central Europe (n=133), The Netherlands (n=9) and Britain (n=37), and 166 individuals from other ancient populations including 118 individuals from Britain who lived both before (n=51) and after (n=67) the arrival of the Beaker Complex (Fig. 1a-b). For genome-wide analyses, we filtered out first-degree relatives and individuals with low coverage (<10,000 SNPs) or evidence of contamination (Methods) and combined our data with previously published ancient DNA data (Extended Data Fig. 2) to form a dataset of 683 ancient samples (Supplementary Table 1). We further merged these data with 2,572 present-day individuals genotyped on the Affymetrix Human Origins array[11,12] and 300 high coverage genomes[13]. To facilitate the interpretation of our genetic results, we also generated 106 new direct radiocarbon dates (Extended Data Table 2; Supplementary Information, section 3).

Y-chromosome analysis

The Y-chromosome composition of Beaker associated males was dominated by R1b-M269 (Supplementary Table 3), a lineage associated with the arrival of Steppe migrants in central Europe during the Late Neolithic/Early Bronze Age[2,3]. Outside Iberia, this lineage was present in 84 out of 90 analysed males. For individuals in whom we could determine the R1b-M269 subtype (n=60), we found that all but two had the derived allele for the R1b-S116/P312 polymorphism, which defines the dominant subtype in western Europe today[14]. In contrast, Beaker-associated individuals from the Iberian Peninsula carried a higher proportion of Y haplogroups known to be common across Europe during the earlier Neolithic period[2,4,15,16], such as I (n=7) and G2 (n=2), while R1b-M269 was found in four individuals (the two with higher coverage could be further classified as R1b-S116/P312). Finding this widespread presence of

the R1b-S116/P312 polymorphism in ancient individuals from central and western Europe suggests that people associated with the Beaker Complex may have had an important role in the dissemination of this lineage throughout most of its present-day distribution.

Genomic insights into the spread of people associated with the Beaker Complex

We performed Principal Component Analysis (PCA) by projecting ancient samples onto a set of present-day populations from West Eurasia and replicate previous findings[11] of two parallel clines, with present-day Europeans on one side and present-day Near Easterners on the other (Extended Data Fig. 3a). Individuals associated with the Beaker Complex are strikingly heterogeneous within the European cline—splayed out along the axis of variation defined by Early Bronze Age Yamnaya Steppe pastoralists at one extreme and Middle Neolithic/Copper Age European farmers at the other extreme (Fig. 1c; Extended Data Fig. 3a)—suggesting that the genetic differentiation may be related to variable amounts of Steppe-related ancestry. We obtained qualitatively consistent inferences using ADMIXTURE model-based clustering[17]. Beaker Complex-associated individuals harboured three main genetic components: one characteristic of European hunter-gatherers, one maximized in Neolithic farmers from the Levant and Anatolia, and one maximized in Neolithic farmers of Iran and present in admixed form in Bronze Age Steppe populations (Extended Data Fig. 3b).

Both PCA and ADMIXTURE are powerful tools for visualizing genetic structure but they do not provide formal tests of admixture between populations. We grouped Beaker Complex individuals based on geographic proximity and genetic similarity (Supplementary Information, section 6), and used *qpAdm*[2] to directly test admixture models and estimate mixture proportions. We modelled their ancestry as a mixture of Mesolithic western European hunter-gatherers (WHG), northwestern Anatolian Neolithic farmers, and Bronze Age Steppe pastoralists (the first two of which contributed to earlier Neolithic Europeans; Supplementary Information, section 8). We find that the great majority of sampled Beaker Complex individuals in areas outside of Iberia (with the exception of Sicily) derive a large portion of their ancestry from populations related to Bronze Age Steppe pastoralists (Fig. 2a), whereas in Iberia, such ancestry is present in only eight of the 39 analysed individuals who represent the earliest detection of Steppe-related genomic affinities in this region. We observe striking differences in ancestry not only at a pan-European scale, but also within regions and even within sites. Unlike other individuals from the Upper Alsace region of France (n=2), an individual from Hégenheim resembles the previous Neolithic populations and can be modelled as a mixture of Anatolian Neolithic and western hunter-gatherers without any Steppe-related ancestry. Given that the radiocarbon date of the Hégenheim individual is older (2832–2476 cal BCE (quoting 95.4% confidence intervals for this and other dates) (Supplementary Information, section 2) than other samples from the same

region (2566–2133 cal BCE), the pattern could reflect temporal differentiation. At Szigetszentmiklós in Hungary, we find Beaker-associated individuals with very different proportions (from 0% to 75%) of Steppe-related ancestry and overlapping dates. This genetic heterogeneity is consistent with early stages of mixture between previously established European Neolithic populations and migrants with Steppe-related ancestry. An implication is that, even at a local scale, the Beaker Complex was associated with people of diverse ancestries.

While the Steppe-related ancestry in Beaker-associated individuals had a recent origin in the East[2,3], the other ancestry component (from previously established European farmers) could potentially be derived from several parts of Europe, as genetically closely related groups were widely distributed during the Neolithic and Copper Ages[2,4,11,16,18–23]. To obtain insight into the origin of this ancestry in Beaker Complex-associated individuals, we began by looking for regional patterns of genetic differentiation within Europe during the Neolithic and Copper Age periods. We examined whether Neolithic and Copper Age test populations predating the emergence of the Beaker Complex shared more alleles with Iberian (*Iberia_EN*) or central European Linearbandkeramik (*LBK_EN*) Early Neolithic populations. As previously described[2], there is genetic affinity to Iberian Early Neolithic farmers in Iberian Middle Neolithic/Copper Age populations, but not in central and northern European Neolithic populations (Fig. 2b), which could be explained by differential affinities to hunter-gatherer individuals from different regions[22] (Extended Data Fig. 4). Neolithic farmers from southern France and Britain are also significantly closer to Iberian Early Neolithic farmers than to central European Early Neolithic farmers (Fig. 2b), consistent with the analysis of a Neolithic farmer genome from Ireland.[23] We ruled out the possibility that these results are driven by similarities in the proportion of hunter-gatherer admixture by modelling Neolithic populations and WHG in an admixture graph framework (Extended Data Fig. 5; Supplementary Information, section 7), and finding that all working models require that a portion of the ancestry of the Neolithic farmers of Britain is derived from groups related to early farmers from Iberia. Megalithic tombs document substantial interaction along the Atlantic façade of Europe, and our results are consistent with such interactions reflecting south-to-north movements of people. More data from southern Britain and Ireland (where currently data are sparse) and nearby regions in continental Europe will be needed to fully understand the complex interactions human movements between Britain, Ireland, and the continent during the Neolithic[24].

The distinctive genetic signatures of pre-Beaker Complex populations in Iberia compared to central Europe allow us to test formally for the origin of the Neolithic farmer-related ancestry in Beaker Complex-associated individuals in our dataset (Supplementary Information, section 8). We grouped individuals from Iberia (n=39) and from outside Iberia (n=172) to increase power, and evaluated the fit of different Neolithic/Copper Age groups with *qpAdm* under the model:

Yamnaya + Neolithic/Copper Age. For Beaker Complex-associated individuals from Iberia, the best fit was obtained when Middle Neolithic and Copper Age populations from the same region were used as a source for their Neolithic farmer-related ancestry, and we could exclude central and northern European populations ($P < 0.0028$) (Fig. 2c). Conversely, the Neolithic farmer-related ancestry in Beaker Complex individuals outside Iberia was most closely related to central and northern European Neolithic populations with relatively high hunter-gatherer admixture (e.g. *Poland_LN*, $P = 0.18$; *Sweden_MN*, $P = 0.25$), and we could significantly exclude Iberian sources ($P < 0.0104$) (Fig. 2c). These results support largely different origins for Beaker Complex-associated individuals, with no discernible Iberia-related ancestry outside Iberia.

Nearly complete turnover of ancestry in Britain

British Beaker Complex-associated individuals (n=19) show strong similarities to central European Beaker Complex-associated individuals in their genetic profile (Extended Data Fig. 3), an observation that is not just restricted to British individuals associated with the 'All Over Corded' Beaker pottery style that is shared between Britain and Central Europe, but also in 3 British individuals associated with the 'Maritime' Beaker pottery style that was the predominant early style in Iberia. The presence of large amounts of Steppe-related ancestry in British Beaker Complex-associated individuals (Fig. 2a) contrasts sharply with Neolithic individuals from Britain (n=51), who have no evidence of Steppe genetic affinities and cluster instead with Middle Neolithic and Copper-Age populations from mainland Europe (Extended Data Fig. 3). Thus, the arrival of Steppe-related ancestry in Britain was mediated by a migration that began with the Beaker Complex. A previous study showed that Steppe-related ancestry arrived in Ireland by the Bronze Age[23], and here we show that – at least in Britain – it arrived earlier in the Copper Age/Beaker period.

Among the different continental Beaker Complex groups analysed in our dataset, individuals from Oostwoud (Province of Noord-Holland, The Netherlands) are the most closely related to the great majority of the Beaker Complex individuals from southern Britain (n=27). They had almost identical Steppe-related ancestry proportions (Fig. 2a), the highest shared genetic drift (Extended Data Fig. 6b) and were symmetrically related to most ancient populations (Extended Data Fig. 6a), showing that they are consistent with being derived from the same ancestral population with limited mixture into either group. This does not necessarily imply that the Oostwoud individuals are direct ancestors of the British individuals, but a genetically closely-related group to the one (perhaps yet to be sampled) that moved into Britain from continental Europe.

We investigated the magnitude of population replacement in Britain with *qpAdm,*[2] modelling the genome-wide ancestry of Copper and Bronze Age individuals (including Beaker Complex-associated individuals) as a mixture of continental Beaker Complex-associated samples (using the Oostwoud individuals as a surrogate) and the British Neolithic population (Supplementary Information, section 8). Fig. 3a shows the results, ordering individuals by date and showing excess Neolithic farmer-related ancestry compared to continental Beaker Complex-associated individuals as a baseline. For the earliest individuals (between ~2400–2000 BCE), the Neolithic ancestry excess is highly variable, consistent with migrant communities that were just beginning to mix with the previously established Neolithic population of Britain. During the subsequent Bronze Age we observe less variation and a modest increase in Neolithic farmer-related ancestry (Fig. 3a), which could represent admixture with persisting British populations with high levels of Neolithic farmer-related ancestry (or alternatively incoming continental populations with higher proportions of Neolithic farmer-related ancestry). In either case, our results imply a minimum of 90±2% local population turnover by the Middle Bronze Age, with no further decrease observed in 5 samples from the Late Bronze Age (Supplementary Information, section 8). While the exact turnover rate and its geographic pattern will be refined with more ancient samples, our results imply that for individuals from Britain during and after the Beaker period, a very high fraction of their DNA derives from ancestors who lived in continental Europe prior to 2400 BCE. An independent line of evidence for population turnover comes from Y-chromosome haplogroup composition. While R1b haplogroups were completely absent in the Neolithic samples (n=33), they represent more than 90% of the Y-chromosomes during Copper and Bronze Age Britain (Fig. 3b; Supplementary Table 3).

Our genetic time transect in Britain also allowed us to track the frequencies of alleles with known phenotypic effects. Derived alleles at rs16891982 (SLC45A2) and rs12913832 (HERC2/OCA2), which contribute to reduced skin and eye pigmentation in Europeans, dramatically increased in frequency between the Neolithic period to the Beaker and Bronze Age periods (Extended Data Fig. 7). Thus, the arrival of migrants associated with the Beaker Complex significantly altered the pigmentation phenotypes of British populations. However, the lactase persistence allele at SNP rs4988235 remained at very low frequencies in our dataset both in Britain and continental Europe, showing that the major increase in its frequency in Britain, as in mainland Europe[3,4,25], occurred in the last 3,500 years.

Discussion

The term 'Bell Beaker' was introduced by late 19th-century and early 20th-century archaeologists to refer to the distinctive pottery style found across western and central Europe at the end of the Neolithic, initially hypothesized to have been spread by a genetically

homogeneous group of people. This idea of a 'Beaker Folk' became unpopular after the 1960s as scepticism about the role of migration in mediating change in archaeological cultures grew[26], although J.G.D. Clark speculated that the Beaker Complex expansion into Britain was an exception[27], a prediction that has now been borne out by ancient genomic data.

Our results prove that the expansion of the Beaker Complex cannot be described by a simple one-to-one mapping of an archaeologically defined material culture to a genetically homogeneous population. This stands in contrast to other archaeological complexes analysed to date, notably the *Linearbandkeramik* first farmers of central Europe[2], the Early Bronze Age Yamnaya of the Steppe[2,3], and to some extent the Corded Ware Complex of central and eastern Europe[2,3]. Instead, our results support a model in which cultural transmission and human migration both played important roles, with the relative balance of these two processes depending on the region. In Iberia, the majority of Beaker-associated individuals lacked Steppe affinities and were genetically most similar to preceding Iberian populations. In central Europe, Steppe-related ancestry was widespread and we can exclude a substantial contribution from Iberian Beaker associated individuals, contradicting initial suggestions of gene flow into central Europe based on analysis of mtDNA[28] and dental morphology[29]. The presence of Steppe-related ancestry in some Iberian individuals demonstrates that gene-flow into Iberia was, however, not uncommon during this period.

Other parts of the Beaker Complex expansion were driven to a substantial extent by migration. This genomic transformation is clearest in Britain due to our dense time transect. The earliest Beaker pots found in Britain show influences from both the lower Rhine region and the Atlantic façade of western Europe[30]. However, such dual influence is not mirrored in the genetic data, as the British Beaker Complex individuals were genetically most similar to lower Rhine individuals from the Netherlands. The arrival of people associated with the Beaker Complex precipitated a profound demographic transformation in Britain, exemplified by the absence of individuals in our dataset without large amounts of Steppe-related ancestry after 2400 BCE. It is possible that the uneven geographic distribution of our samples, coupled with different burial practises between local and incoming populations (cremation versus burial) during the early stages of interaction could result in a sampling bias against local individuals. However, the signal observed during the Copper Age/Beaker period persisted, without any evidence of genetically Neolithic-like individuals among the 67 Bronze Age individuals we newly report. These results are notable in light of strontium and oxygen isotope analyses of British skeletons from the Beaker and Bronze Age periods[31], which have provided no evidence of substantial mobility over individuals' lifetimes from locations with cooler climates or from places with geologies atypical of Britain. However, the isotope data are only sensitive to first-generation migrants, and do not rule out movements from regions such as the lower Rhine, which is

consistent with the genetic data, or from other geologically similar regions for which DNA sampling is still sparse. Further sampling of regions on the European continent may reveal additional candidate sources.

By analysing DNA data from ancient individuals we have been able to provide constraints on the processes underlying cultural and social changes in Europe during the third millennium BCE. Our results motivate further archaeological research to identify the changes in social organization, technology, subsistence, climate, population sizes[32] or pathogen exposure[33,34] that could have precipitated the demographic changes uncovered in this study.

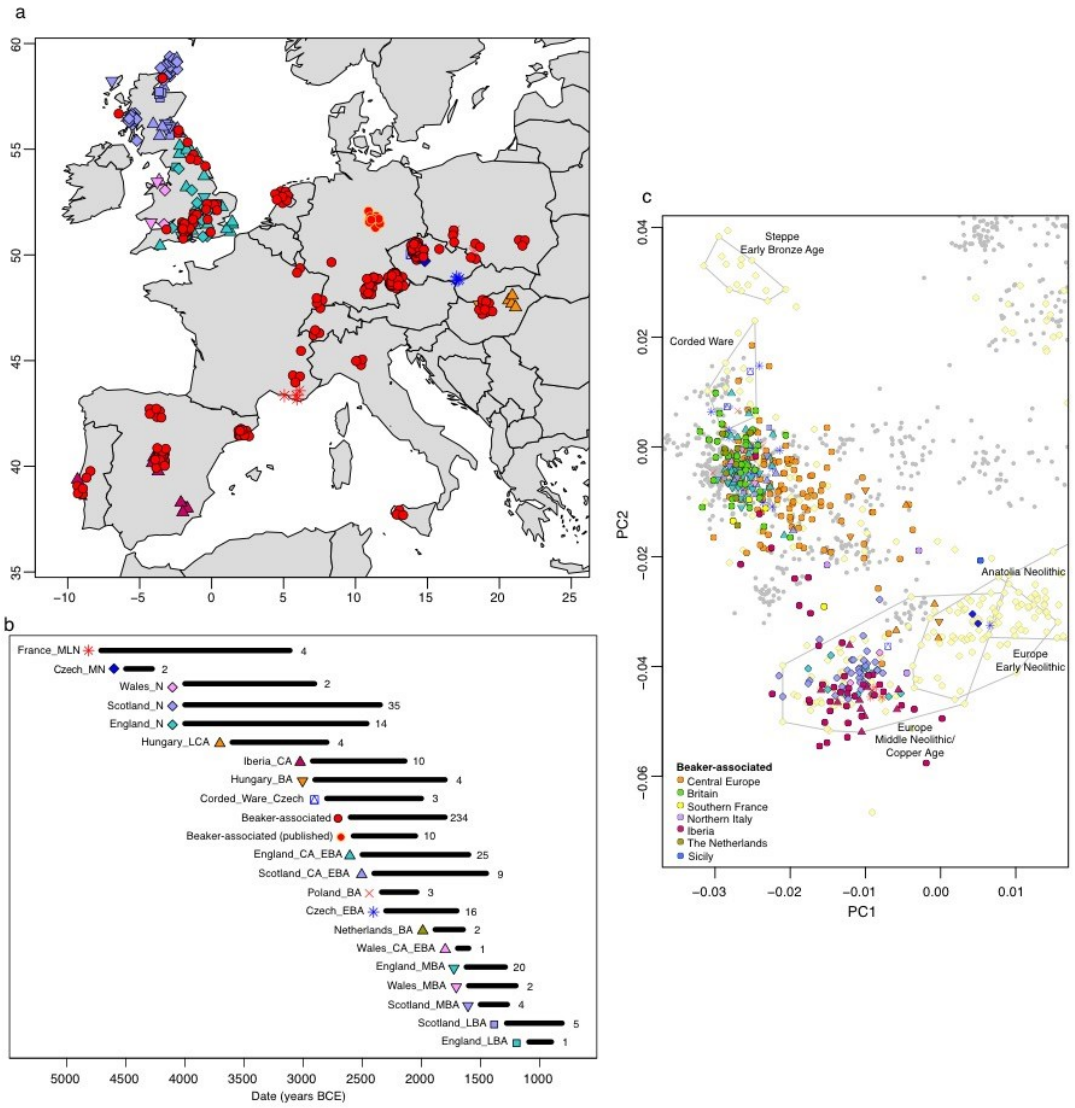

Figure 1. Spatial, temporal, and genetic structure of individuals in this study. a, Geographic distribution of samples with new genome-wide data. For clarity, random jitter was added for sites with multiple individuals. **b**, Time ranges for samples with new genome-wide data. Sample sizes are given next to each bar. **c**, Principal component analysis of 990 present-day West Eurasian individuals (grey dots), with previously published (pale yellow) and new ancient samples projected onto the first two principal components. This figure is a zoom of Extended Data Fig 3a. E, Early; M, Middle; L, Late; N, Neolithic; CA, Copper Age; BA, Bronze Age.

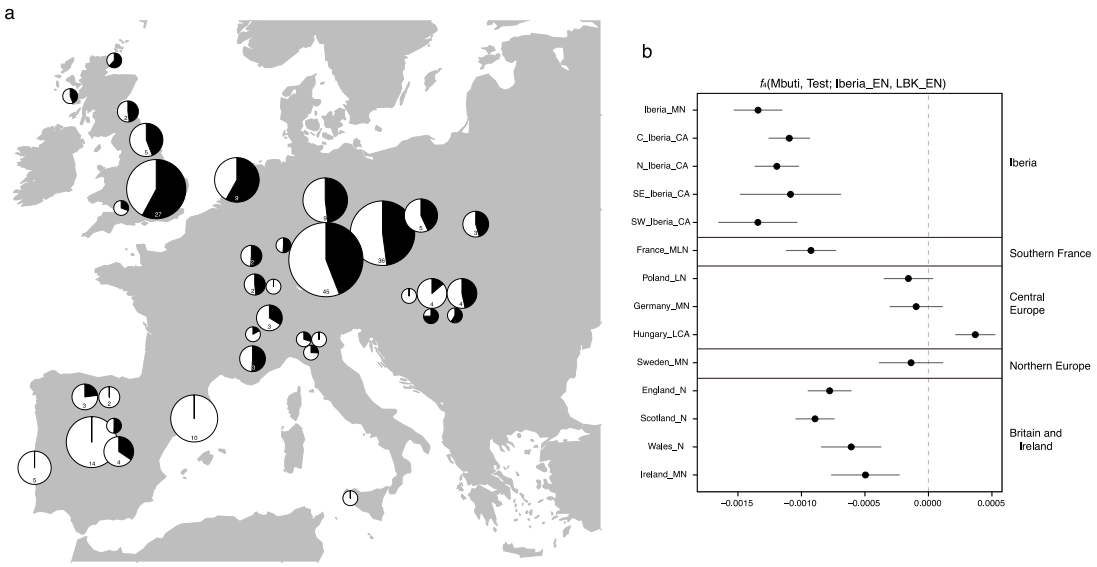

c

		Neolithic/Copper Age source pop									
		Iberia_MN	C_Iberia_CA	N_Iberia_CA	SE_Iberia_CA	SW_Iberia_CA	Germany_MN	Poland_LN	Hungary_LCA	Sweden_MN	France_MLN
Test pop	BC Iberia combined	1.46E-01	6.58E-01	3.49E-05	1.31E-01	5.64E-01	3.01E-12	4.99E-07	5.09E-70	2.78E-03	2.96E-02
	BC outside Iberia combined	1.11E-12	6.31E-10	2.18E-10	9.93E-03	1.04E-02	2.51E-13	1.84E-01	6.05E-55	2.45E-01	4.61E-04

Figure 2. Investigating the genetic makeup of Beaker Complex individuals. a, Proportion of Steppe-related ancestry (shown in black) in Beaker Complex-associated groups, computed with *qpAdm* under the model Steppe_EBA + Anatolia_N + WHG. The area of the pie is proportional to the number of individuals (shown inside the pie if more than one). See Supplementary Information, section 8 for mixture proportions and standard errors. **b**, *f*-statistics of the form f_4(Mbuti, *Test*; Iberia_EN, LBK_EN) computed for European populations before the emergence of the Beaker Complex. The statistic takes negative values if the *Test* shares more alleles with Iberia_EN (positive values in the case of excess affinity with LBK_EN). Error bars represent ±1 standard errors. **c**, Testing different populations as a source for the Neolithic ancestry component in Beaker Complex individuals. The table shows the P-values (highlighted if >0.05) for the model: Steppe_EBA + Neolithic/Copper Age source population. BC, Beaker complex; E, Early; M, Middle; L, Late; N, Neolithic; CA, Copper Age; BA, Bronze Age; N_Iberia, Northern Iberia; C_Iberia, Central Iberia; SE_Iberia, Southeast Iberia; SW_Iberia, Southwest Iberia.

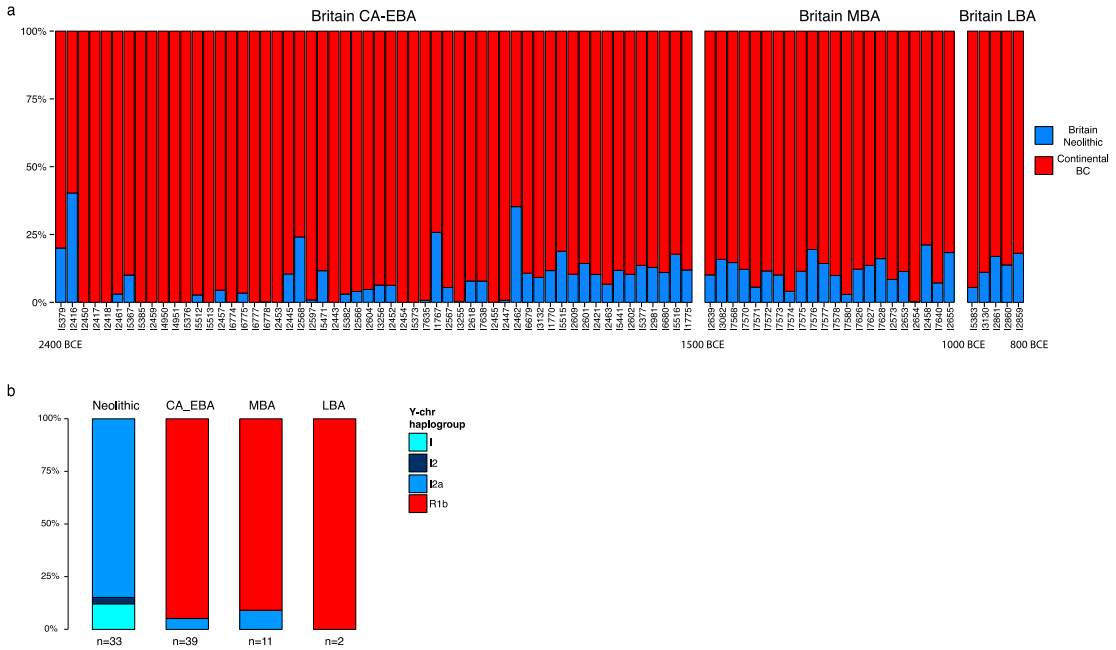

Figure 3. Population transformation in Britain associated with the arrival of the Beaker Complex. **a,** Modelling Copper and Bronze Age (including Beaker Complex) individuals from Britain as a mixture of continental Beaker Complex-associated individuals (red, represented by Beaker Complex samples from Oostwoud) and the Neolithic population from Britain (blue). Individuals are ordered chronologically (oldest on the left) and included in the plot if represented by more than 100,000 SNPs. See Supplementary Information, section 8 for mixture proportions and standard errors. **b**, Y-chromosome haplogroup composition in males from Britain. CA, Copper Age; EBA, Early Bronze Age; MBA, Middle Bronze Age; LBA, Late Bronze Age. BC, Beaker complex**.**

References

1. Czebreszuk, J. Bell Beakers from West to East. in *Ancient Europe, 8000 B.C. to A.D. 1000: An Encyclopedia of the Barbarian World* (eds. Bogucki, P. I. & Crabtree, P. J.) 476–485 (Charles Scribner's Sons, 2004).
2. Haak, W. *et al.* Massive migration from the steppe was a source for Indo-European languages in Europe. *Nature* **522,** 207–211 (2015).
3. Allentoft, M. E. *et al.* Population genomics of Bronze Age Eurasia. *Nature* **522,** 167–172 (2015).
4. Mathieson, I. *et al.* Genome-wide patterns of selection in 230 ancient Eurasians. *Nature* **528,** 499–503 (2015).
5. Czebreszuk, J. Similar But Different. Bell Beakers in Europe. *Adam Mickiewicz University* (2004).
6. Cardoso, J. L. Absolute chronology of the Beaker phenomenon North of the Tagus estuary : demographic and social implications. *Trabajos de Prehistoria* **71,** 56–75 (2014).
7. Jeunesse, C. The dogma of the Iberian origin of the Bell Beaker: attempting its deconstruction. *J. Neolit. Archaeol.* **16,** 158–166 (2015).
8. Fokkens, H. & Nicolis, F. *Background to Beakers. Inquiries into regional cultural backgrounds of the Bell Beaker complex*. (Leiden: Sidestone Press, 2012).
9. Vander Linden, M. What linked the Bell Beakers in third millennium BC Europe? *Antiquity* **81,** 343–352 (2007).
10. Fu, Q. *et al.* An early modern human from Romania with a recent Neanderthal ancestor. *Nature* **524,** 216–219 (2015).
11. Lazaridis, I. *et al.* Ancient human genomes suggest three ancestral populations for present-day Europeans. *Nature* **513,** 409–413 (2014).
12. Lazaridis, I. *et al.* Genomic insights into the origin of farming in the ancient Near East. *Nature* **536,** 1–22 (2016).
13. Mallick, S. *et al.* The Simons Genome Diversity Project: 300 genomes from 142 diverse populations. *Nature* **538,** (2016).
14. Valverde, L. *et al.* New clues to the evolutionary history of the main European paternal lineage M269: dissection of the Y-SNP S116 in Atlantic Europe and Iberia. *Eur. J. Hum. Genet.* 1–5 (2015). doi:10.1038/ejhg.2015.114
15. Gamba, C. *et al.* Ancient DNA from an Early Neolithic Iberian population supports a pioneer colonization by first farmers. *Mol. Ecol.* **21,** 45–56 (2012).
16. Günther, T. *et al.* Ancient genomes link early farmers from Atapuerca in Spain to modern-day Basques. *Proc. Natl. Acad. Sci. U. S. A.* **112,** 11917–11922 (2015).
17. Alexander, D. H., Novembre, J. & Lange, K. Fast model-based estimation of ancestry in unrelated individuals. *Genome Res.* **19,** 1655–1664 (2009).
18. Broushaki, F. *et al.* Early Neolithic genomes from the eastern Fertile Crescent. *Science* **7943,** 1–16 (2016).
19. Skoglund, P. *et al.* Genomic Diversity and Admixture Differs for Stone-Age Scandinavian Foragers and Farmers. *Science* **201,** 786–792 (2014).
20. Olalde, I. *et al.* A Common Genetic Origin for Early Farmers from Mediterranean Cardial and Central European LBK Cultures. *Mol. Biol. Evol.* **32,** 3132–3142 (2015).
21. Mathieson, I. *et al.* The Genomic History of Southeastern Europe. *bioRxiv* (2017).
22. Lipson, M. *et al.* Parallel ancient genomic transects reveal complex population history of early European farmers. *bioRxiv* (2017).
23. Cassidy, L. M. *et al.* Neolithic and Bronze Age migration to Ireland and establishment of the insular Atlantic genome. *Proc. Natl. Acad. Sci. U. S. A.* **113,** 1–6 (2016).
24. Sheridan, J. A. The Neolithisation of Britain and Ireland: the big picture. in *Landscapes in transition* (eds. Finlayson, B. & Warren, G.) 89–105 (Oxbow, Oxford, 2010).
25. Burger, J., Kirchner, M., Bramanti, B., Haak, W. & Thomas, M. G. Absence of the lactase-persistence-associated allele in early Neolithic Europeans. *Proc. Natl. Acad. Sci. U. S. A.* **104,** 3736–41 (2007).
26. Clarke, D. L. The Beaker network: social and economic models. in *Glockenbecher*

Symposion,Oberried, 18–23 März 1974 (eds. Lanting, J. N. & DerWaals, J. D. van) 460–77 (1976).
27. Clark, G. The Invasion Hypothesis in British Archaeology. *Antiquity* **40,** 172–189 (1966).
28. Brotherton, P. *et al.* Neolithic mitochondrial haplogroup H genomes and the genetic origins of Europeans. *Nat. Commun.* **4,** 1764 (2013).
29. Desideri, J. When Beakers Met Bell Beakers : an analysis of dental remains. *British archaeological Reports - International Series; 2292* (2011).
30. Needham, S. Transforming Beaker Culture in North-West Europe; Processes of Fusion and Fission. *Proc. Prehist. Soc.* **71,** 171–217 (2005).
31. Parker Pearson, M. *et al.* Beaker people in Britain: migration, mobility and diet. *Antiquity* **90,** 620–637 (2016).
32. Shennan, S. *et al.* Regional population collapse followed initial agriculture booms in mid-Holocene Europe. *Nat. Commun.* **4,** 2486 (2013).
33. Valtueña, A. A. *et al.* The Stone Age Plague : 1000 years of Persistence in Eurasia. *bioRxiv* (2016).
34. Rasmussen, S. *et al.* Early Divergent Strains of Yersinia pestis in Eurasia 5,000 Years Ago. *Cell* **163,** 571–582 (2015).
35. Dabney, J. *et al.* Complete mitochondrial genome sequence of a Middle Pleistocene cave bear reconstructed from ultrashort DNA fragments. *Proc. Natl. Acad. Sci. U. S. A.* **110,** 15758–63 (2013).
36. Damgaard, P. B. *et al.* Improving access to endogenous DNA in ancient bones and teeth. *Sci. Rep.* **5,** 11184 (2015).
37. Korlević, P. *et al.* Reducing microbial and human contamination in dna extractions from ancient bones and teeth. *Biotechniques* **59,** 87–93 (2015).
38. Rohland, N., Harney, E., Mallick, S., Nordenfelt, S. & Reich, D. Partial uracil – DNA – glycosylase treatment for screening of ancient DNA. *Philos. Trans. R. Soc. London B* (2015). doi:10.1098/rstb.2013.0624
39. Briggs, A. W. *et al.* Removal of deaminated cytosines and detection of in vivo methylation in ancient DNA. *Nucleic Acids Res.* **38,** 1–12 (2010).
40. Maricic, T., Whitten, M. & Pääbo, S. Multiplexed DNA sequence capture of mitochondrial genomes using PCR products. *PLoS One* **5,** e14004 (2010).
41. Kircher, M., Sawyer, S. & Meyer, M. Double indexing overcomes inaccuracies in multiplex sequencing on the Illumina platform. *Nucleic Acids Res.* **40,** 1–8 (2012).
42. Behar, D. M. *et al.* A 'Copernican' reassessment of the human mitochondrial DNA tree from its root. *Am. J. Hum. Genet.* **90,** 675–84 (2012).
43. Li, H. & Durbin, R. Fast and accurate short read alignment with Burrows–Wheeler transform. *Bioinformatics* **25,** 1754–1760 (2009).
44. Fu, Q. *et al.* A revised timescale for human evolution based on ancient mitochondrial genomes. *Curr. Biol.* **23,** 553–9 (2013).
45. Sawyer, S., Krause, J., Guschanski, K., Savolainen, V. & Pääbo, S. Temporal patterns of nucleotide misincorporations and DNA fragmentation in ancient DNA. *PLoS One* **7,** e34131 (2012).
46. Korneliussen, T. S., Albrechtsen, A. & Nielsen, R. ANGSD : Analysis of Next Generation Sequencing Data. *BMC Bioinformatics* **15,** 1–13 (2014).
47. Li, H. *et al.* The Sequence Alignment/Map format and SAMtools. *Bioinformatics* **25,** 2078–9 (2009).
48. Weissensteiner, H. *et al.* HaploGrep 2: mitochondrial haplogroup classification in the era of high-throughput sequencing. *Nucleic Acids Res.* **44,** W58-63 (2016).
49. van Oven, M. & Kayser, M. Updated comprehensive phylogenetic tree of global human mitochondrial DNA variation. *Hum. Mutat.* **30,** E386-94 (2009).
50. Patterson, N. *et al.* Ancient admixture in human history. *Genetics* **192,** 1065–93 (2012).
51. Raghavan, M. *et al.* Upper Palaeolithic Siberian genome reveals dual ancestry of Native Americans. *Nature* **505,** 87–91 (2014).
52. Orlando, L. *et al.* Recalibrating Equus evolution using the genome sequence of an early

Middle Pleistocene horse. *Nature* **499,** 74–8 (2013).
53. Gallego Llorente, M. *et al.* Ancient Ethiopian genome reveals extensive Eurasian admixture in Eastern Africa. *Science* **350,** 820–822 (2015).
54. Fu, Q. *et al.* The genetic history of Ice Age Europe. *Nature* **534,** 200–205 (2016).
55. Kilinc, G. M. *et al.* The Demographic Development of the First Farmers in Anatolia. *Curr. Biol.* **26,** 1–8 (2016).
56. Gallego-Llorente, M. *et al.* The genetics of an early Neolithic pastoralist from the Zagros, Iran. *Sci. Rep.* **6,** 4–10 (2016).
57. Olalde, I. *et al.* Derived immune and ancestral pigmentation alleles in a 7,000-year-old Mesolithic European. *Nature* **507,** 225–8 (2014).
58. Hofmanová, Z. *et al.* Early farmers from across Europe directly descended from Neolithic Aegeans. *Proc. Natl. Acad. Sci. U. S. A.* **113,** 6886–6891 (2016).
59. Patterson, N., Price, A. L. & Reich, D. Population structure and eigenanalysis. *PLoS Genet.* **2,** e190 (2006).
60. Purcell, S. *et al.* PLINK : A Tool Set for Whole-Genome Association and Population-Based Linkage Analyses. *Am. J. Hum. Genet.* **81,** 559–575 (2007).
61. Busing, F. M. T. A., Meijer, E. & Van Der Leeden, R. Delete- m Jackknife for Unequal m. *Stat. Comput.* **9,** 3–8 (1999).
62. Rojo-Guerra, M. Á., Kunst, M., Garrido-Pena, R. & García-Martínez de Lagrán, I. Morán-Dauchez, G. Un desafío a la eternidad. Tumbas monumentales del Valle de Ambrona. *Memorias Arqueología en Castilla y León 14, Junta de Castilla y León, Valladolid* (2005).
63. Gamba, C. *et al.* Genome flux and stasis in a five millennium transect of European prehistory. *Nat. Commun.* **5,** 5257 (2014).

Methods

Ancient DNA analysis

We screened skeletal samples for DNA preservation in dedicated clean rooms. We extracted DNA[35–37] and prepared barcoded next generation sequencing libraries, the majority of which were treated with uracil-DNA glycosylase to greatly reduce the damage (except at the terminal nucleotide) that is characteristic of ancient DNA[38,39] (Supplementary Information, section 4). We initially enriched libraries for sequences overlapping the mitochondrial genome[40] and ~3000 nuclear SNPs using synthesized baits (CustomArray Inc.) that we PCR amplified. We sequenced the enriched material on an Illumina NextSeq instrument with 2x76 cycles, and 2x7 cycles to read out the two indices[41]. We merged read pairs with the expected barcodes that overlapped by at least 15 bases, mapped the merged sequences to hg19 and to the reconstructed mitochondrial DNA consensus sequence[42] using the *samse* command in bwa (v0.6.1)[43], and removed duplicated sequences. We evaluated DNA authenticity by estimating the rate of mismatching to the consensus mitochondrial sequence[44], and also requiring that the rate of damage at the terminal nucleotide was at least 3% for UDG-treated libraries[44] and 10% for non-UDG-treated libraries[45].

For libraries that were promising after screening, we enriched in two consecutive rounds for sequences overlapping 1,233,013 SNPs ('1240k SNP capture')[2,10] and sequenced 2x76 cycles and 2x7 cycles on an Illumina NextSeq500 instrument. We processed the data bioinformatically as for the mitochondrial capture data, this time mapping only to the human reference genome *hg19* and merging the data from different libraries of the same individual. We further evaluated authenticity by studying the ratio of X-to-Y chromosome reads and estimating X-chromosome contamination in males based on the rate of heterozygosity[46]. Samples with evidence of contamination were either filtered out or restricted to sequences with terminal cytosine deamination to remove sequences that derived from modern contaminants. Finally, we filtered out from our genome-wide analysis dataset samples with fewer than 10,000 targeted SNPs covered at least once and samples that were first-degree relatives of others in the dataset (keeping the sample with the larger number of covered SNPs) (Supplementary Table 1).

Mitochondrial haplogroup determination

We used the mitochondrial capture bam files to determine the mitochondrial haplogroup of each sample with new data, restricting to sequences with MAPQ≥30 and base quality ≥30. First, we constructed a consensus sequence with samtools and bcftools[47], using a majority rule and requiring a minimum coverage of 2. We called haplogroups with HaploGrep2[48] based on

phylotree[49] (mtDNA tree Build 17 (18 Feb 2016)). Mutational differences compared to the rCRS and corresponding haplogroups can be viewed in Supplementary Table 2.

Y-chromosome analysis

We determined Y-chromosome haplogroups for both new and published samples (Supplementary Information, section 5). We made use of the sequences mapping to 1240k Y-chromosome targets, restricting to sequences with mapping quality ≥30 and bases with quality ≥30. We called haplogroups by determining the most derived mutation for each sample, using the nomenclature of the International Society of Genetic Genealogy (http://www.isogg.org) version 11.110 (21 April 2016). Haplogroups and their supporting derived mutations can be viewed in Supplementary Table 3.

Merging newly generated data with published data

We assembled two datasets for genome-wide analyses:

- *HO* includes 2,572 present-day individuals from worldwide populations genotyped on the Human Origins Array[11,12,50] and 683 ancient individuals. The ancient set includes 211 Beaker Complex individuals (195 newly reported, 7 with shotgun data[3] for which we generated 1240k capture data and 9 previously published[3,4]), 68 newly reported individuals from relevant ancient populations and 298 previously published[12,18,19,21–23,51–58] individuals (Supplementary Table 1). We kept 591,642 autosomal SNPs after intersecting autosomal SNPs in the 1240k capture with the analysis set of 594,924 SNPs from Lazaridis et al.[11].

-*HOIll* includes the same set of ancient samples and 300 present-day individuals from 142 populations sequenced to high coverage as part of the Simons Genome Diversity Project[13]. For this dataset, we used 1,054,671 autosomal SNPs, excluding SNPs of the 1240k array located on sex chromosomes or with known functional effects.

For each individual, we represented the allele at each SNP by randomly sampling one sequence, discarding the first and the last two nucleotides of each sequence.

Principal component analysis

We carried out principal component analysis (PCA) on the *HO* dataset using the *smartpca* program in EIGENSOFT[59]. We computed principal components on 990 present-day West Eurasians and projected ancient individuals using lsqproject: YES and shrinkmode: YES.

ADMIXTURE analysis

We performed model-based clustering analysis using ADMIXTURE[17] on the *HO* reference dataset, including 2,572 present-day individuals from worldwide populations and the ancient individuals. First, we carried out LD-pruning on the dataset using PLINK[60] with the flag --indep-pairwise 200 25 0.4, leaving 306,393 SNPs. We ran ADMIXTURE with the cross validation (--cv) flag specifying from K=2 to K=20 clusters, with 20 replicates for each value of K and keeping for each value of K the replicate with highest log likelihood. In Extended Data Fig. 3b we show the cluster assignments at K=8 of newly reported individuals and other relevant ancient samples for comparison. We chose this value of K as it was the lowest one for which components of ancestry related both to Iranian farmers and European hunter-gatherers were maximized.

***f*-statistics**

We computed *f*-statistics on the *HOIll* dataset using ADMIXTOOLS[50] with default parameters (Supplementary Information, section 6). We used *qpDstat* with f4mode:Yes for f_4-statistics and *qp3Pop* for outgroup *f*3-statistics. We computed standard errors using a weighted block jackknife[61] over 5 Mb blocks.

Inference of mixture proportions

We estimated ancestry proportions on the *HOIll* dataset using *qpAdm*[2] and a basic set of 9 *Outgroups*: Mota, Ust_Ishim, MA1, Villabruna, Mbuti, Papuan, Onge, Han, Karitiana. For some analyses (Supplementary Information, section 8) we added additional outgroups to this basic set.

Admixture graph modelling

We modelled the relationships between populations in an Admixture Graph framework with the software *qpGraph* in ADMIXTOOLS[50], using the *HOIll* dataset and Mbuti as an outgroup (Supplementary Information, section 7).

Allele frequency estimation from read counts

We used allele counts at each SNP to perform maximum likelihood estimation of allele frequencies in ancient populations as in ref.[4]. In Extended Data Fig. 7, we show derived allele frequency estimates at three SNPs of functional importance for different ancient populations.

Data availability

All 1240k and mitochondrial capture sequencing data are available from the European Nucleotide Archive, accession number XXXXXXXX [to be made available on publication].
The genotype dataset we analysed is available from the Reich Lab website at [to be made available on publication].

Acknowledgements

We thank D. Anthony, J. Koch, I. Mathieson and C. Renfrew for comments and critiques. We thank A. C. Sousa for providing geographical information on a Portuguese sample. We thank A. Martín Cólliga from Generalitat de Catalunya and L. Loe for help in contacting archaeologists. We thank M. Giesen for assisting with samples selection. We thank the Museo Arqueológico Regional de la Comunidad de Madrid for kindly allowing access to samples from Camino de las Yeseras. We thank the Hunterian Museum, University of Glasgow, for allowing access to samples from sites in Scotland, and particularly to Dr. S.-A. Coupar for help in accessing material. We thank the Museu Municipal de Torres Vedras for allowing the study and sampling of Cova da Moura collection. We are grateful to the Orkney Museum for allowing access to samples from Orkney, and particularly to G. Drinkall for facilitating this work. We thank the Great North Museum: Hancock, the Society of Antiquaries of Newcastle upon Tyne, and Sunderland Museum for sharing samples. We are grateful to E. Willerslev for sharing several dozen samples that were analyzed in this study and for supporting several co-authors at the Centre for GeoGenetics at the University of Copenhagen who worked on this project. We are grateful for institutional support (grant RVO:67985912) from the Institute of Archaeology, Czech Academy of Sciences. G.K. was supported by Momentum Mobility Research Group of the Hungarian Academy of Sciences. This work was supported by the Wellcome Trust [100713/Z/12/Z]. D.F. was supported by an Irish Research Council grant GOIPG/2013/36. P.W.S., J.K. and A.M. were supported by the Heidelberg Academy of Sciences (WIN project 'Times of Upheaval'). C.L.-F. was supported by a grant from FEDER and Ministry of Economy and Competitiveness (BFU2015-64699-P) of Spain. D.R. was supported by US National Science Foundation HOMINID grant BCS-1032255, US National Institutes of Health grant GM100233, and is an investigator of the Howard Hughes Medical Institute. Radiocarbon work at Penn State was supported by the NSF Archaeometry (BCS-1460369, D.J.K.) and Archaeology (BCS-1725067, D.J.K and T. H.) programs.

Author Contributions

S.B., M.E.A, N.R., A.S.-N., A.M., N.B., M.F., E.H., M.M., J.O., K.S., O.C., F.C., R.P., J.K., W.H., I.B. and D.R. performed or supervised wet laboratory work. G.T.C. and D.J.K. undertook the radiocarbon dating of a large fraction of the British samples. I.A., K.K., A.B., K.W.A.,

A.A.F., E.B., M.B.-B., D.B., C.B., C.Bo., L.B., T.A., L.Bü., S.C., L.C.N., O.E.C., G.C., B.C., A.D., K.E.D., N.D., M.E., C.E., M.K., J.F.F., H.F., C.F., M.G., R.G.P., M.H.-U., E.Had., G.H., N.J., T.K., K.M., S.P., P.L., O.L., A.L., J.L.M., T.M., J.I.M, K.Mc., M.B.G., A.Mo., G.K., V.K., A.C., R.Pa., A.E., K.Kö., T.H., T.S., J.D., M.H., D.K., P.V., M.D., F.B., R.F.F., A. H.-C., S.T., E.C., L.L., A.V., A.Z., C.W., G.D., E.G.-D., B.N., M.B., M.Lu., R.M., J.De., M.Be., G.B., M.Fu., J.L.C., C.L., M.P.P., P.W., T.D.P., P.P., P.-J.R., P.R., R.R., M.A.R.G., A.S., J.S., A.M.S., V.S., L.V., J.Z., D.C., T.Hi., V.H., A.Sh., K.-G.S., P.W.S., R.P., J.K., W.H., I.B., C.L.-F. and D.R. assembled archaeological material. I.O., S.M., T.B., A.M., E.A., M.L., I.L., N.P., Y.D., Z.F., D.F., P.d.K., T.K.H., M.G.T. and D.R. analysed or supervised analysis of data. I.O., C.L.-F. and D.R. wrote the manuscript with input from all co-authors.

Supplementary Tables

Supplementary Table 1. Ancient individuals included in this study.

Supplementary Table 2. Mitochondrial haplogroup calls for individuals with newly reported data.

Supplementary Table 3. Y-chromosome calls for males with newly reported data.

Supplementary Table 4. Radiocarbon database.

Extended Data Figure 1. **Beaker complex artefacts**. **a**, Beaker and flint implements excavated at Newmill, Perth and Kinross District, Tayside Region, Scotland. **b**, Beaker Complex grave goods from La Sima III barrow, Soria, Spain[62]. Photo: Alejandro Plaza, Museo Numantino.

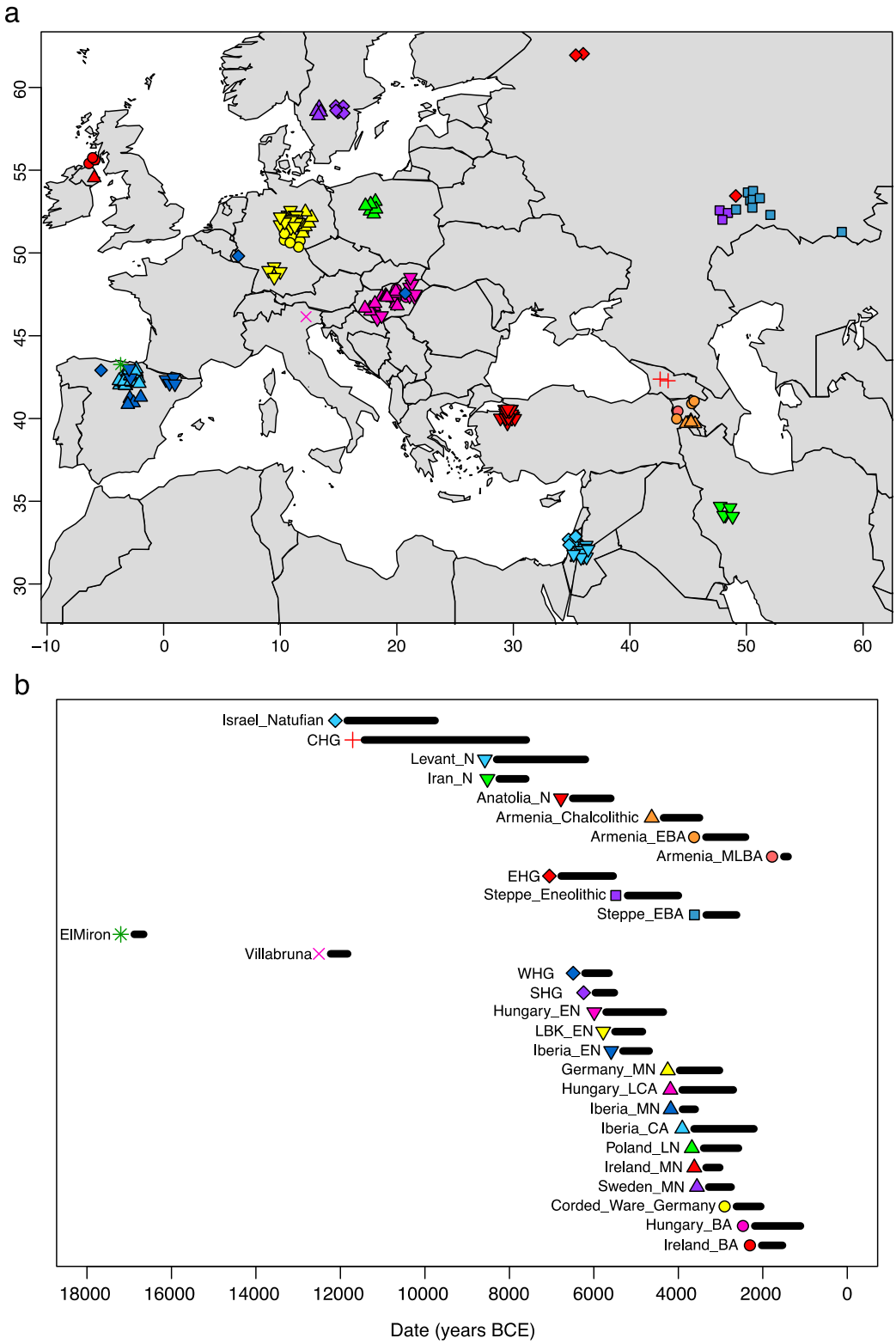

Extended Data Figure 2. **Ancient individuals with previously published genome-wide data used in this study**. **a,** Sampling locations. **b**, Time ranges. W/E/S/CHG, Western/Eastern/Scandinavian/Caucasus hunter-gatherers; E, Early; M, Middle; L, Late; N, Neolithic; CA, Copper Age; BA, Bronze Age.

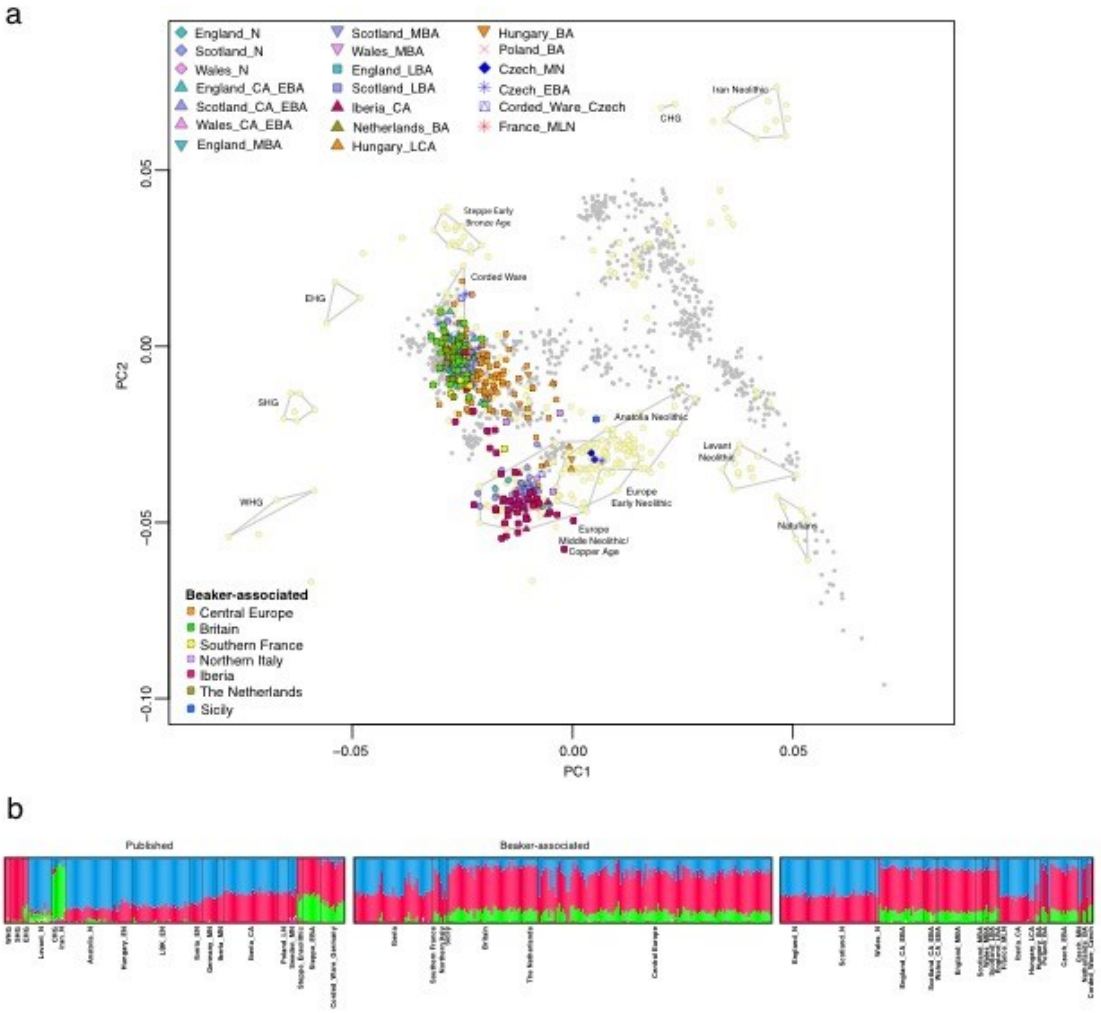

Extended Data Figure 3. Population structure. a, Principal component analysis of 990 present-day West Eurasian individuals (grey dots), with previously published (pale yellow) and new ancient samples projected onto the first two principal components. **b**, ADMIXTURE clustering analysis with k=8 showing ancient individuals. W/E/S/CHG, Western/Eastern/Scandinavian/Caucasus hunter-gatherers; E, Early; M, Middle; L, Late; N, Neolithic; CA, Copper Age; BA, Bronze Age.

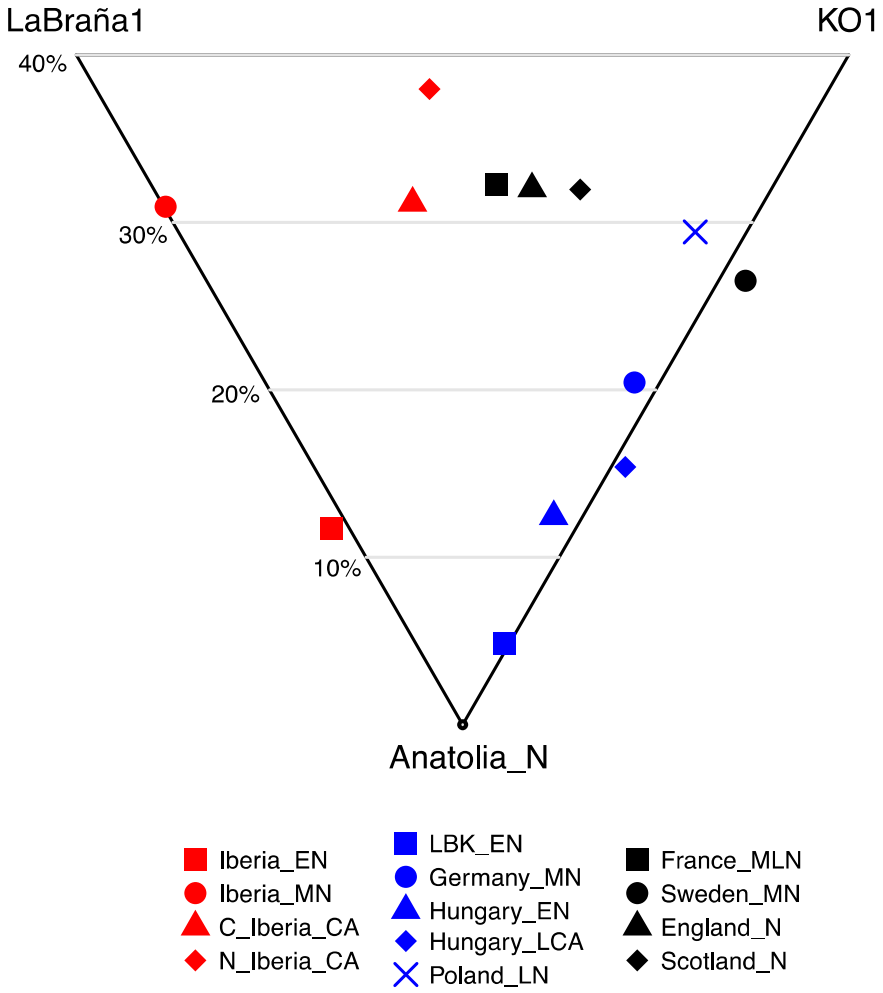

Extended Data Figure 4. **Hunter-gatherer affinities in Neolithic/Copper Age Europe**. Differential affinity to hunter-gatherer individuals (LaBraña1[57] from Spain and KO1[63] from Hungary) in European populations before the emergence of the Beaker Complex. See Supplementary Information, section 8 for mixture proportions and standard errors computed with *qpAdm*. E, Early; M, Middle; L, Late; N, Neolithic; CA, Copper Age; BA, Bronze Age; N_Iberia, Northern Iberia; C_Iberia, Central Iberia.

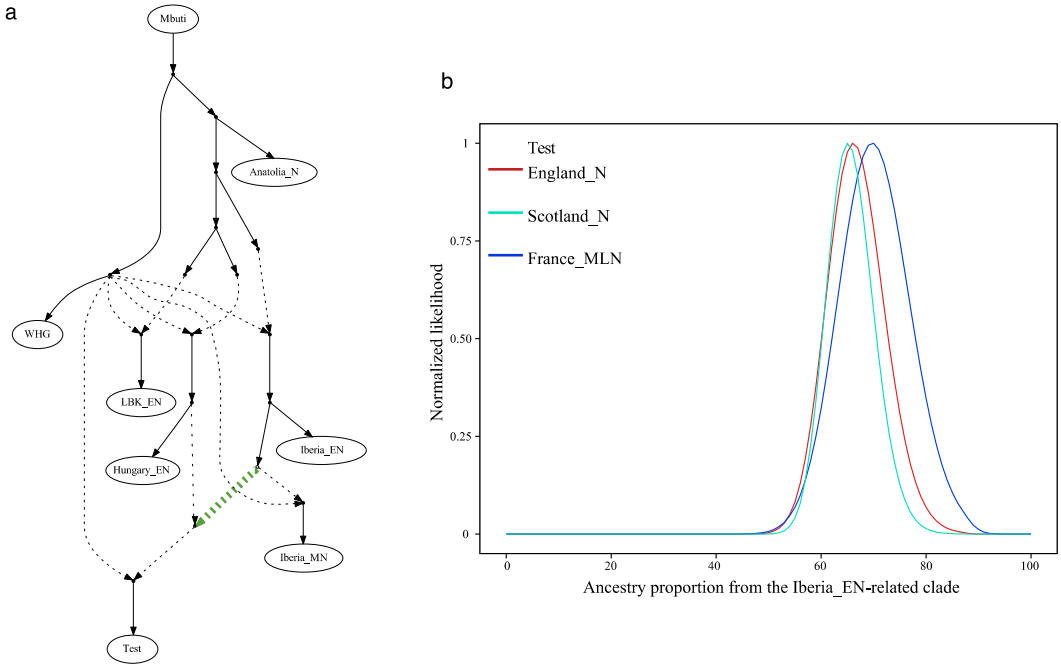

Extended Data Figure 5. **Modelling the relationships between Neolithic populations**. **a,** Admixture graph fitting a *Test* population as a mixture of sources related to both Iberia_EN and Hungary_EN. **b,** Likelihood distribution for models with different proportions of the source related to Iberia_EN (green admixture edge in (a)) when *Test* is England_N, Scotland_N or France_MLN.

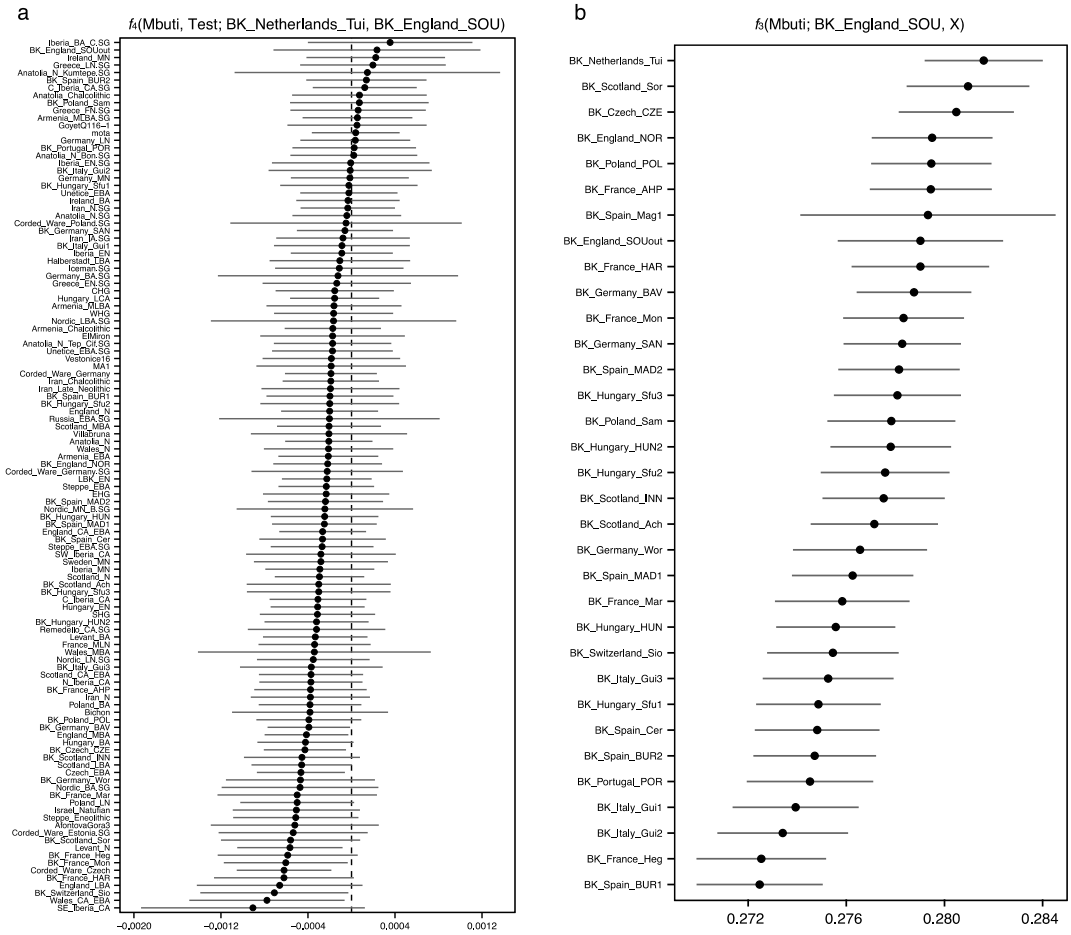

Extended Data Figure 6. **Genetic affinity between Beaker Complex-associated individuals from southern England and the Netherlands**. **a**, *f*-statistics of the form f_4(Mbuti, Test; BK_Netherlands_Tui, BK_England_SOU). Negative values indicate that Test is closer to BK_Netherlands_Tui than to BK_England_SOU, and the opposite for positive values. Error bars represent ±3 standard errors. **b**, Outgroup-f_3 statistics of the form f_3(Mbuti; BK_England_SOU, X) measuring shared genetic drift between BK_England_SOU and other Beaker Complex groups. Error bars represent ±1 standard errors.

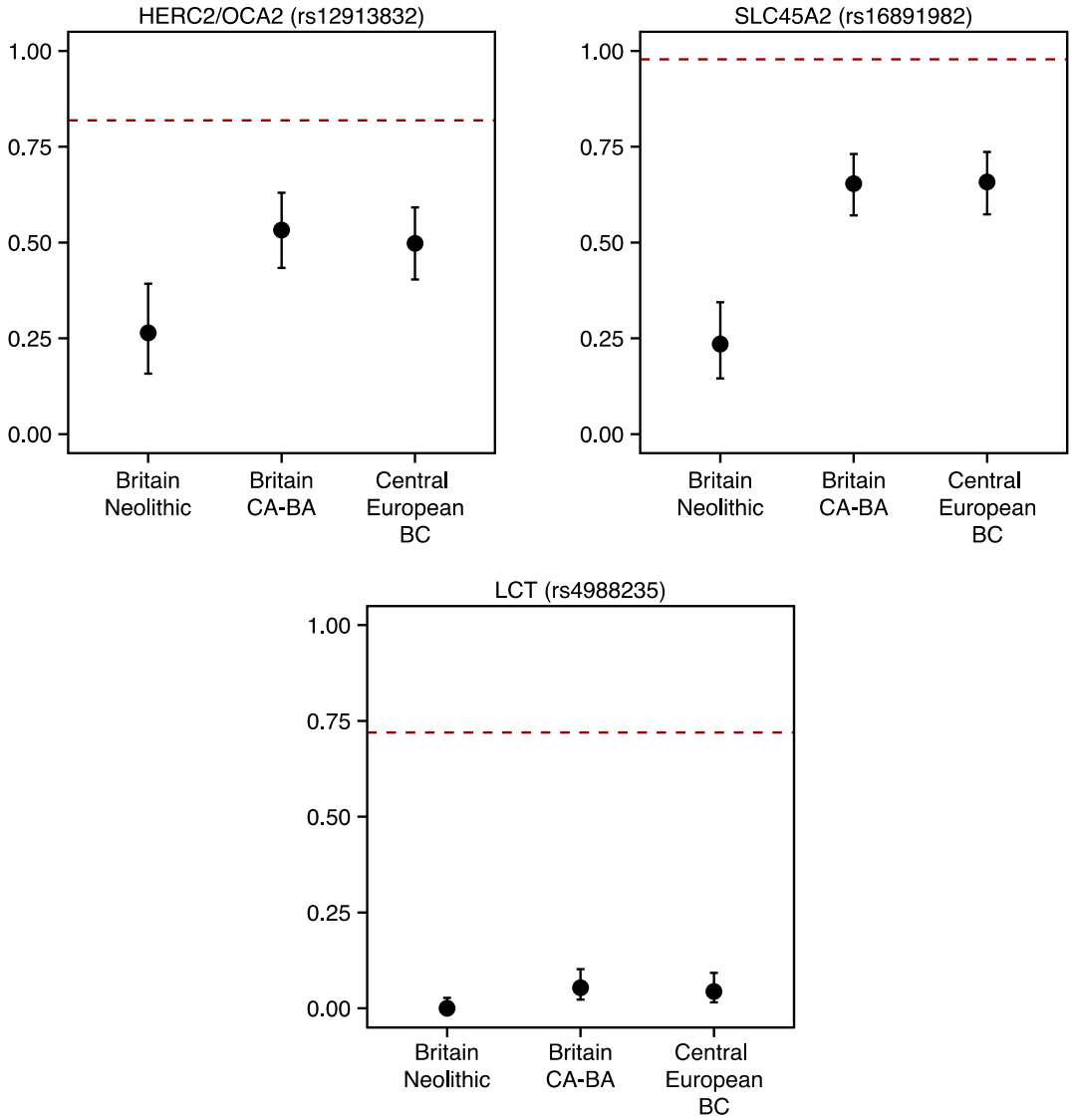

Extended Data Figure 7. Derived allele frequencies at three SNPs of functional importance. Error bars represent 1.9-log-likelihood support interval. The red dashed lines show allele frequencies in the 1000 Genomes GBR population (present-day people from Great Britain). BC, Beaker Complex; CA, Copper Age; BA, Bronze Age.

Extended Data Table 1. Sites with new genome-wide data reported in this study.

Site	N	Approx. date range (BCE)	Country
Brandysek	12	2500–2000	Czech Republic
Kněževes	2	2500–1900	Czech Republic
Lochenice	1	2500–1900	Czech Republic
Lovosice II	1	2500–1900	Czech Republic
Moravska Nova Ves	4	2300–1900	Czech Republic
Prague 5 - Mala Ohrada	14	2500–2200	Czech Republic
Prague 5, Jinonice	14	2500–1700	Czech Republic
Prague 8, Kobylisy, Ke Stírce Street	12	2500–1900	Czech Republic
Radovesice	13	2500–2000	Czech Republic
Velké Přílepy	3	2500–1900	Czech Republic
Clos de Roque, Saint Maximin-la-Sainte-Baume	3	4700–4500	France
Collet Redon, La Couronne-Martigues	1	3500–3100	France
Hégenheim Necropole, Haut-Rhin	1	2800–2500	France
La Fare, Forcalquier	1	2500–2200	France
Marlens, Sur les Barmes, Haute-Savoie	1	2500–2100	France
Mondelange, PAC de la Sente, Moselle	2	2400–1900	France
Rouffach, Haut-Rhin	1	2300–2100	France
Sierentz, Les Villas d'Aurele, Haut-Rhin	2	2600–2300	France
Villard, Lauzet-Ubaye	2	2200–1900	France
Alburg-Lerchenhaid, Spedition Häring, Bavaria	13	2500–2100	Germany
Augsburg Sportgelände, Augsburg	6	2500–2000	Germany
Hugo-Eckener-Straße, Augsburg	3	2500–2000	Germany
Irlbach, County of Straubing-Bogen, Bavaria	17	2500–2000	Germany
Künzing-Bruck, Lkr. Deggendorf, Bavaria	3	2500–2000	Germany
Landau an der Isar, Bavaria	5	2500–2000	Germany
Manching-Oberstimm, Bavaria	2	2500–2000	Germany
Osterhofen-Altenmarkt, Bavaria	4	2600–2000	Germany
Unterer Talweg 58-62, Augsburg	2	2500–2200	Germany
Unterer Talweg 85, Augsburg	1	2400–2100	Germany
Weichering, Bavaria	4	2800–1800	Germany
Worms-Herrnsheim, England	1	2800–1800	Germany
Aberdour Road, Dunfermline, Fife, Scotland	1	2000–1800	Great Britain
Abingdon Spring Road cemetery, Oxfordshire, England	1	2500–2200	Great Britain
Achavanich, Wick, Scotland	1	2500–2100	Great Britain
Amesbury Down, Wiltshire, England	13	2500–1300	Great Britain
Banbury Lane, Northamptonshire, England	3	3400–3100	Great Britain
Barrow Hills, Radley, Oxfordshire, England	1	2300–1800	Great Britain
Barton Stacey, Hampshire, England	1	2200–2000	Great Britain
Baston and Langtoft, South Lincolnshire, England	2	1700–1600	Great Britain
Biddenham Loop, Bedfordshire, England	9	1600–1300	Great Britain
Boatbridge Quarry, Thankerton, Scotland	1	2400–2100	Great Britain
Boscombe Airfield, Wiltshire, England	1	1800–1600	Great Britain
Canada Farm, Sixpenny Handley, Dorset, England	2	2500–2300	Great Britain
Carsington Pasture Cave, Derbyshire, England	2	3700–2000	Great Britain
Central Flying School, Upavon, Wiltshire, England	1	2500–1800	Great Britain
Cissbury, Sussex, England	1	3600–3400	Great Britain
Clachaig, Scotland	1	3500–3400	Great Britain
Clay Farm, Cambridgeshire, England	2	1400–1300	Great Britain
Covesea Cave 2, Scotland	3	2100–800	Great Britain
Covesea Caves, Scotland	2	1000–800	Great Britain
Culverhole Cave, West Glamorgan, Wales	1	1600–1200	Great Britain
Dairy Farm, Willington, England	1	2300–1900	Great Britain
Distillery Cave, Scotland	3	3800–3400	Great Britain
Ditchling Road, England	1	2500–1900	Great Britain
Doune, Perth and Kinross, Scotland	1	1800–1600	Great Britain
Dryburn Bridge, Scotland	2	2300–1900	Great Britain
Eton Rowing Course, Buckinghamshire, England	2	3600–2900	Great Britain
Eweford Cottages, Scotland	1	2100–1900	Great Britain
Flying School, Netheravon, Wiltshire, England	2	2500–1800	Great Britain
Fussell's Lodge, Salisbury, Wiltshire, England	2	3800–3600	Great Britain
Giggleswick Scar, Kelco Cave, North Yorkshire,	1	3700–3500	Great Britain
Great Orme Mines, Llandudno, North Wales	1	1700–1600	Great Britain
Hasting Hill, Sunderland, Tyne and Wear, England	2	2500–1800	Great Britain
Hexham Golf Course, Northumberland, England	1	2000–1800	Great Britain
Holm of Papa Westray North, Scotland	4	3500–3100	Great Britain
Isbister, Orkney, Scotland	10	3300–2300	Great Britain
Leith, Merrilees Close, City of Edinburgh, Scotland	2	1600–1500	Great Britain
Longniddry, Evergreen House, Coast Road , Scotland	3	1500–1300	Great Britain

Longniddry, Grainfoot, Scotland	1	1300–1000	Great Britain
Low Hauxley, Northumberland, England	2	2100–1600	Great Britain
Macarthur Cave, Scotland	1	4000–3800	Great Britain
Melton Quarry, East Riding of Yorkshire, England	1	1900–1700	Great Britain
Neale's Cave, Paington, Somerset, England	1	2000–1600	Great Britain
North Face Cave, Llandudno, North Wales	1	1400–1200	Great Britain
Nr. Ablington, Figheldean, England	1	2500–1800	Great Britain
Nr. Millbarrow, Wiltshire, England	1	3600–3400	Great Britain
Over Narrows, Needingworth Quarry, England	5	2200–1300	Great Britain
Pabay Mor, Scotland	1	1400–1300	Great Britain
Point of Cott, Orkney, Scotland	2	3700–3100	Great Britain
Porton Down, Wiltshire, England	2	2500–1900	Great Britain
Quoyness, Scotland	1	3100–2900	Great Britain
Raschoille Cave, Oban, Argyll and Bute, Scotland	9	4000–2900	Great Britain
Raven Scar Cave, Ingleton, North Yorkshire, England	1	1100–900	Great Britain
Reaverhill, Barrasford, Northumberland, England	1	2100–2000	Great Britain
Rhos Ddigre, Denbighshire, Wales	1	3100–2900	Great Britain
River Thames Skulls, Mortlake, London, England	1	1900–1700	Great Britain
River Thames Skulls, Syon Reach, London, England	1	2500–2100	Great Britain
Sorisdale, Coll, Scotland	1	2500–2100	Great Britain
Staxton Beacon, Staxton,England	1	2400–1600	Great Britain
Stenchme, Lop Ness, Orkney, Scotland	1	2000–1500	Great Britain
Summerhill,Blaydon, Tyne and Wear, England	1	1900–1700	Great Britain
Thanet, Kent, England	4	2100–1700	Great Britain
Thurston Mains, Innerwick, East Lothian, Scotland	1	2300–2000	Great Britain
Tinkinswood, Glamorgan, Wales	1	4000–3300	Great Britain
Totty Pot, Cheddar, Somerset, England	1	2800–2500	Great Britain
Trumpington Meadows, Cambridge, England	2	2200–2000	Great Britain
Tulach an t'Sionnach, Scotland	1	3700–3500	Great Britain
Tulloch of Assery A, Scotland	1	3700–3400	Great Britain
Tulloch of Assery B, Scotland	1	3800–3600	Great Britain
Turners Yard, Fordham, Cambridgeshire, England	1	1700–1500	Great Britain
Unstan Chamber Tomb, Orkney, Scotland	1	3400–2800	Great Britain
Upper Swell, Chipping Norton, Gloucestershire,	1	4000–3500	Great Britain
Waterhall Farm, Chippenham, Cambridgeshire, England	1	2000–1700	Great Britain
West Deeping, Lincolnshire, England	1	2300–2000	Great Britain
Whitehawk, Brighton, Sussex, England	1	3700–3500	Great Britain
Wick Barrow, England	1	2500–1900	Great Britain
Wilsford, England	2	2500–1900	Great Britain
Windmill Fields, Ingleby Barwick, England	4	2300–2000	Great Britain
Yarnton, Oxfordshire, England	4	2500–1900	Great Britain
Budakalász, Csajerszke (M0 Site 12)	2	2600–2200	Hungary
Budapest-Békásmegyer	3	2500–2100	Hungary
Mezöcsát-Hörcsögös halom alatt	4	2800–2400	Hungary
Szigetszentmiklós-Vízműtelep Üdülősor	4	2900–1800	Hungary
Szigetszentmiklós,Felső Ürge-hegyi dűlő	6	2500–2200	Hungary
Pergole 2, Partanna, Sicily	3	2500–1900	Italy
Via Guidorossi, Parma, Emilia Romagna	3	2200–1900	Italy
Dzielnica	1	2300–2000	Poland
Iwiny	1	2300–2000	Poland
Jordanów Śląski	1	2300–2200	Poland
Kornice	4	2500–2100	Poland
Racibórz-Stara Wieś	1	2300–2000	Poland
Samborzec	3	2500–2100	Poland
Strachów	1	2000–1800	Poland
Żerniki Wielkie	1	2300–2100	Poland
Bolores, Estremadura	1	2800–2600	Portugal
Cova da Moura, Torres Vedras	1	2300–2100	Portugal
Galeria da Cisterna, Almonda	2	2500–2200	Portugal
Verdelha dos Ruivos, District of Lisbon	3	2700–2300	Portugal
Arroyal I, Burgos	5	2600–2200	Spain
Camino de las Yeseras, Madrid	14	2800–1700	Spain
Camino del Molino, Caravaca, Murcia	4	2900–2100	Spain
Humanejos, Madrid	11	2900–2000	Spain
La Magdalena, Madrid	3	2800–1800	Spain
Paris Street, Cerdanyola, Barcelona	10	2900–2300	Spain
Virgazal, Tablada de Rudrón, Burgos	1	2300–2000	Spain
Sion-Petit-Chasseur, Dolmen XI	3	2500–2000	Switzerland
De Tuithoorn, Oostwoud, Noord-Holland	11	2600–1600	The Netherlands

Extended Data Table 2. 106 newly reported radiocarbon dates

Sample	Date	Location	Country
I4145	2279–2033 calBCE (3740±35 BP, Poz-84460)	Kněževes	Czech Republic
I1392	2832–2476 calBCE (4047±29 BP, MAMS-25935)	Hégenheim Necropole, Haut-Rhin	France
I4144	2572–2512 calBCE (3955±35 BP, Poz-84553)	Osterhofen-Altenmarkt	Germany
E09537_d	2471–2300 calBCE (3909±29 BP, MAMS 29074)	Unterer Talweg 58-62, Augsburg, Bavaria	Germany
I4249	2336-2141 calBCE (3802±26 BP, BRAMS1217)	Irlbach LKR	Germany
E09538	2464–2212 calBCE (3870±30 BP, MAMS 29075)	Unterer Talweg 58-62, Augsburg, Bavaria	Germany
I3592	2458-2204 calBCE (3844±33 BP, BRAMS-1218)	Alburg-Lerchenhaid, Spedition Häring, Bavaria	Germany
I4250	2434-2150 calBCE (3825±26 BP, BRAMS1219)	Irlbach LKR	Germany
I3593	2398-2146 calBCE (3817±26 BP, BRAMS-1215)	Alburg-Lerchenhaid, Spedition Häring, Bavaria	Germany
I3590	2339-2143 calBCE (3802±26 BP, BRAMS-1217)	Alburg-Lerchenhaid, Spedition Häring, Bavaria	Germany
I2657	3952–3781 calBCE (5052±30 BP, SUERC-68701)	Macarthur Cave	Great Britain
I2633	3766-3642 calBCE (4911±32 BP, SUERC-68634)	Tulloch of Assery B	Great Britain
I2659	3762–3644 calBCE (4914±27 BP, SUERC-68702)	Distillery Cave	Great Britain
I2691	3701–3640 calBCE (4881±25 BP, SUERC-68704)	Distillery Cave	Great Britain
I2796	3706–3536 calBCE (4856±33 BP, SUERC-69074)	Point of Cott, Orkney	Great Britain
I2634	3704–3535 calBCE (4851±34 BP, SUERC-68638)	Tulach an t'Sionnach	Great Britain
I2635	3653–3390 calBCE (4796±37 BP, SUERC-68639)	Tulloch of Assery A	Great Britain
I2636	3520–3362 calBCE (4651±33 BP, SUERC-68640)	Holm of Papa Westray North	Great Britain
I2988	3517–3362 calBCE (4645±29 BP, SUERC-68711)	Clachaig	Great Britain
I2660	3514–3353 calBCE (4631±29 BP, SUERC-68703)	Distillery Cave	Great Britain
I2650	3500–3360 calBCE (4754±36 BP, SUERC-68642)	Holm of Papa Westray North	Great Britain
I2637	3510–3340 calBCE (4697±33 BP, SUERC-68641)	Holm of Papa Westray North	Great Britain
I2605	3632–3373 calBCE (4710±35 BP, Poz-83483)	Eton Rowing Course	Great Britain
I2980	3361–3102 calBCE (4530±33 BP, SUERC-69073)	Point of Cott, Orkney	Great Britain
I2651	3330–3090 calBCE (4525±36 BP, SUERC-68643)	Holm of Papa Westray North	Great Britain
I3085	3339–3027 calBCE (4471±29 BP, SUERC-68724)	Isbister, Orkney	Great Britain
I2978	3336–3024 calBCE (4464±29 BP, SUERC-68725)	Isbister, Orkney	Great Britain
I2934	3327–3036 calBCE (4466±33 BP, SUERC-69071)	Isbister, Orkney	Great Britain
I2935	3336–3012 calBCE (4451±29 BP, SUERC-68723)	Isbister, Orkney	Great Britain
I2979	3334–2942 calBCE (4447±29 BP, SUERC-68726)	Isbister, Orkney	Great Britain
I2631	3098–2907 calBCE (4384±36 BP, SUERC-68633)	Quoyness	Great Britain
I2933	3011–2886 calBCE (4309±29 BP, SUERC-68722)	Isbister, Orkney	Great Britain
I2977	3009–2764 calBCE (4275±33 BP, SUERC-69072)	Isbister, Orkney	Great Britain
I2630	2581–2464 calBCE (3999±32 BP, SUERC-68632)	Isbister, Orkney	Great Britain
I2932	2571–2348 calBCE (3962±29 BP, SUERC-68721)	Isbister, Orkney	Great Britain
I2612	2465–2209 calBCE (3865±35 BP, Poz-83492)	Hasting Hill, Sunderland, Tyne and Wear	Great Britain
I2416	2470-2285 calBC (3830±30 BP, Beta-432804)	Amesbury Down, Wiltshire	Great Britain
I2418	2440–2200 calBCE (3835±25 BP, NZA-32788)	Amesbury Down, Wiltshire	Great Britain
I2565	2470–2140 calBCE (3829±38 BP, OxA-13562)	Amesbury Down, Wiltshire	Great Britain
I2459	2460–2140 calBCE (3829±30 BP, SUERC-54823)	Amesbury Down, Wiltshire	Great Britain
I2457	2480-2280 calBCE (3890±30 BP, SUERC-36210)	Amesbury Down, Wiltshire	Great Britain
I2457	2200-2031 calBCE (3717±28 BP, SUERC-69975)	Amesbury Down, Wiltshire	Great Britain
I2453	2289–2041 calBCE (3760±35 BP, Poz-83404)	West Deeping	Great Britain
I2445	2137–1930 calBCE (3650±35 BP, Poz-83407)	Yarnton	Great Britain
I2596	2280–2030 calBCE (3739±30 BP, NZA-32484)	Amesbury Down, Wiltshire	Great Britain
I2566	2210–2030 calBCE (3734±25 BP, NZA-32490)	Amesbury Down, Wiltshire	Great Britain
I2452	2195–1920 calBCE (3700±30 BP, Beta-444979)	Dairy Farm, Willington	Great Britain
I2452	2277–2030 calBCE (3735±35 BP, Poz-83405)	Dairy Farm, Willington	Great Britain
I2598	2140–1940 calBCE (3664±30 BP, NZA-32494)	Amesbury Down, Wiltshire	Great Britain
I2460	2030–1820 calBCE (3575±27 BP, SUERC-53041)	Amesbury Down, Wiltshire	Great Britain
I2609	2023–1772 calBCE (3560±40 BP, Poz-83423)	Hexham Golf Course, Northumberland	Great Britain
I2610	1936–1746 calBCE (3515±35 BP, Poz-83498)	Summerhill,Blaydon, Tyne and Wear	Great Britain
I1775	1693–1600 calBCE (3344±27 BP, OxA-14308)	Great Orme Mines, Llandudno, North Wales	Great Britain
I2574	1415–1228 calBCE (3065±36 BP, SUERC-62072)	North Face Cave, Llandudno, North Wales	Great Britain
I2786	2459–2206 calBCE (3850±35 BP, Poz-83639)	Szigetszentmiklós,Felső Ürge-hegyi dűlő	Hungary
I2787	2458–2202 calBCE (3840±35 BP, Poz-83640)	Szigetszentmiklós,Felső Ürge-hegyi dűlő	Hungary
I2741	2458–2154 calBCE (3835±35 BP, Poz-83641)	Szigetszentmiklós,Felső Ürge-hegyi dűlő	Hungary
I4229	2289–2135 calBCE (3775±25 BP, PSU-1750)	Cova da Moura	Portugal
I0826	2833–2480 calBCE (4051±28 BP, MAMS-25940)	Paris Street, Cerdanyola, Barcelona	Spain
I0257	2571–2350 calBCE (3965±29 BP, MAMS-25937)	Paris Street, Cerdanyola, Barcelona	Spain
I0462	2566–2346 calBCE (3950±26 BP, MAMS-25936)	Arroyal I, Burgos	Spain
I0825	2474–2300 calBCE (3915±29 BP, MAMS-25939)	Paris Street, Cerdanyola, Barcelona	Spain